Wavelength tuning and emission width widening of ultrabroad quantum dash interband laser

C. L. Tan, H. S. Djie,[a] Y. Wang,[b] C. E. Dimas, V. Hongpinyo, Y. H. Ding, and B. S. Ooi[c]
Center for Optical Technologies and Department of Electrical and Computer Engineering, Lehigh University, Bethlehem, Pennsylvania 18015, USA

(Received 13 July 2008; accepted 23 August 2008; published online 15 September 2008)

The authors report the demonstration of the bandgap-tuned InAs quantum dash broadband laser with widened laser emission linewidth at room temperature using postgrowth intermixing technique. The 100 nm wavelength blueshifted, as-cleaved laser exhibits ultrabroad lasing spectral coverage of ~85 nm at a center wavelength of 1.54 μm with a total emission power of ~1 W per device. Compared to the as-grown laser, this laser shows broader lasing bandwidth (~41 nm) with improved spectral ripple (<1 dB). © *2008 American Institute of Physics*.
[DOI: 10.1063/1.2981578]

Self-assembled nanostructures have been gaining wide interest in the fabrication of semiconductor lasers and amplifiers due to their vastly improved optoelectronic characteristics.[1–3] Due to quasi-three-dimensional carrier confinement and intrinsic properties, Qdash enables several interesting laser diode characteristics such as improved temperature insensitivity, optical feedback resistance, wide spectral tunability, and broad stimulated emission.[1,4,5] In addition, the gain properties of a Qdash amplifier bear the distinct fingerprint of a quantum-wire-like density of states,[3] while gain recovery characteristics and recovery time constants resemble QD characteristics.[6] Moreover, it has been proposed that the role of optical gain broadening,[7] which results in broadband emission from QD lasers, is also inherent in Qdash lasers. These unique features will help to overcome the challenges in the nanoscaled epitaxial engineering of highly inhomogeneous QD for broadband laser applications.

In this letter, we demonstrate the widened broadband laser emission of Qdash laser[5] by using impurity-free vacancy disordering (IFVD) technique. Wavelength blueshift and linewidth broadening after postgrowth intermixing pave a way to the realization of monolithically integrated ultrabroadband Qdash laser with extended wavelength coverage, with applications in optical telecommunication, chemical sensor systems, atmospheric or planetary gases, high-precision optical metrology and spectroscopy, and biomedical imaging.[5] Furthermore, the high power emission of ~1 W per device can be potentially employed as a high efficient resonant pumping source for eye-safe Er-doped amplifiers and solid-state lasers.

The Qdash laser structure comprises four sheets of 5 ML InAs dashes, each of which is embedded within a 7.6 nm thick compressively strained $In_{0.64}Ga_{0.16}Al_{0.2}As$ QW and a 30 nm thick tensile-strained $In_{0.50}Ga_{0.32}Al_{0.18}As$ quantum barrier layer.[5] A 475 nm thick SiO_2 was first deposited on samples. The IFVD process is performed by annealing the SiO_2 capped sample at 750 °C in nitrogen ambient for 1 min in a rapid thermal processor. During the annealing, the SiO_2 cap will enhance preferential atomic outdiffusion, hence enhancing group-III atomic interdiffusion in the Qdash active region and resulting in the effective bandgap modification of Qdash.[8] Photoluminescence (PL) spectroscopy using a 980 nm diode laser as an excitation source was performed at 77 K after the dielectric cap removal. Standard broad area lasers with 50 μm wide oxide stripes were then fabricated from the intermixed samples. Current injection was performed to the non-facet-coated lasers at 0.2% duty cycle.

Carriers localized in different dots/dashes have shown interesting phenomena of lasing spectra.[5,9] This unique feature of dot/dash can be well studied from the evolution of state-filling spectroscopy at 77 K under different excitations (Fig. 1). At low excitation, 3 W/cm^2, the ground state emissions of 1.57 and 1.50 μm are dominant in the as-grown (AG) and the intermixed samples, respectively. The PL spectra are gradually broadened in both samples with increasing excitation. Under the same excitation density, the PL linewidth of the intermixed sample is wider. At the excitation of 1500 W/cm^2, the PL linewidth increases by 11 nm (from 94 to 111 nm) after the intermixing process. The phenomenon of carrier localization in Qdash becomes evident when the intermixed sample shows a larger variation in full width at half maximum (ΔFWHM up to 47 nm) than the AG (up to 18 nm) under various excitations relative to the FWHM obtained at 3 W/cm^2 (inset of Fig. 1).

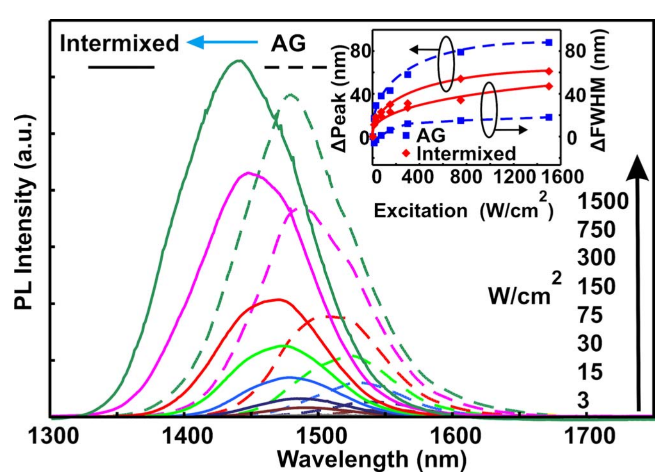

FIG. 1. (Color online) The PL spectra of both as-grown and intermixed samples show global blueshift after intermixing. The inset shows the corresponding changes of FWHM and PL peak wavelength as compared to those obtained under optical excitation of 3 W/cm^2.

[a]Present address: JDS Uniphase Corporation, San Jose, California 95134.
[b]Present address: OptiComp Corporation, Zephyr Cove, Nevada 89448.
[c]Author to whom correspondence should be addressed. Electronic mail: bsooi@lehigh.edu.

The enormously large broadening of the PL spectra is attributed to the contribution of multiple transition states[5] with large inhomogeneous broadening of the noninteracting Qdash ensembles.[6] This observation is clearly different from that of QD[8] and conventional QW structures. The IFVD technique is generally well known to improve the size homogeneity of semiconductor nanostructure system and hence smaller variation in energy transition after intermixing. For instance, at the excitation of 1500 W/cm^2, the PL linewidth decreases by 6 nm after the IFVD process is performed by annealing the SiO_2 capped sample at 750 °C for 2 min.[10] However, the opposite observations of larger PL linewidth after intermediate intermixing suggests the presence of different interdiffusion rates at given intermixing degree in the Qdash nanostructures. The presence of more noninteracting Qdash will contribute to radiative recombination emission over larger wavelength coverage and thus a larger FWHM in PL spectra. Nevertheless, both intermixed and AG Qdash samples showing saturation of ΔFWHM at excitation over 400 W/cm^2 indicates large degeneracy levels in highly confined energy states of Qdash, similar to QD nanostructures.[11]

Furthermore, the integrated PL intensity increases after intermixing. This observation is contrary to conventional quantum-confined nanostructures, which can be attributed to the continuous PL wavelength blueshift observed in both AG and intermixed samples with increasing optical excitation densities. The continuous blueshifts of the PL peak wavelength up to 88 nm in the AG sample and 61 nm in the intermixed sample at the excitation of 1500 W/cm^2, relative to those obtained at 3 W/cm^2, are shown in the inset of Fig. 1. The effect of band filling is not sufficient to explain a significant blueshift. Hence, it is reasonably ascribed to the postulation of continuum states[6] in the Qdash nanostructures. Continuum states serve as an effective medium for exciton scattering and thus change the dephasing rate[7] at each energy level within the highly inhomogeneous ensembles. The wide distribution of energy levels due to the nature of inhomogeneous Qdash (FWHM of 76 nm from the PL measurement of AG sample at low excitation of 3 W/cm^2) will further serve as the radiative recombination states or "sink" for the scattered excitons from the dense continuum states. Consequently, ultrabroadband lasing spectra of the diode laser fabricated from these samples are observed, which will be discussed later. Nevertheless, smaller blueshift of PL peak wavelength in the intermixed sample, as depicted in the inset of Fig. 1, indicates that IFVD enhances the Qdash inhomogeneity more so in larger sizes of Qdashes. Assuming a uniform injection of group-III vacancies from the surface during the IFVD process, the interdiffusion in the vertical direction will affect the dash height more than other directions.[12] At an intermediate stage of intermixing, the thick dash family, where the quantized energy level located closer to the conduction band minima, will experience a larger degree of intermixing as the effective height or thickness of the dash decreases. In addition, the local effective concentration for the thick dash family is higher than that for the thin dashes. Under uniform annealing temperature, the thick Qdash family that has a larger interdiffusion length will yield larger degree of intermixing. As a result, the largest wavelength blueshift (~65 nm) is observed at the excitation of 3 W/cm^2 (dominant emission from thick dashes) as compared to the smaller blueshift (~38 nm) at the excitation of 1500 W/cm^2 (dominant emission from thin dashes).

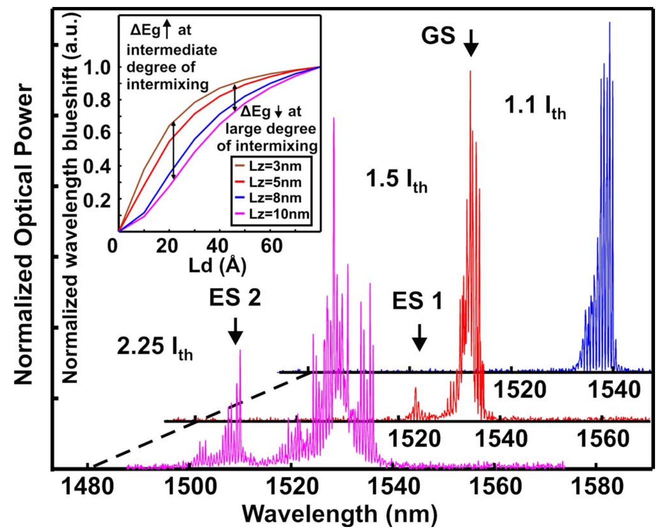

FIG. 2. (Color online) The lasing spectra show the changes of multistate emission from ground state (GS), first excited state (ES 1), and second excited state (ES 2) of the intermixed device, under different current injections of $1.1I_{th}$, $1.5I_{th}$, and $2.25I_{th}$. The inset shows the blueshift of normalized transition wavelength when the diffusion length increases in one-dimensional quantum-confined structure with different well widths (L_z).

The solution of the diffusion problem in the Qdash can be estimated by an equivalent one-dimensional quantum-confined model (transverse direction of vacancy interdiffusion) by assuming a substance of concentration C_0, confined in a region of n repeating well and barrier of width w and b, respectively, centered at zero that is given by

$$C_n = \frac{C_0}{2}\left\{ 2 - \sum_{n=1}^{k}\left[\mathrm{erf}\left(\frac{x-(n-1)(w+b)}{2L_D}\right) + \mathrm{erf}\left(\frac{x-[nw+(n-1)b]}{2L_D}\right)\right]\right\}. \quad (1)$$

The origin of the x coordinate is at the left barrier of the first well. Four repeating wells and barriers with arbitrary width are used to calculate the confined ground state (GS). The chosen material system is not critical because it serves only as a reference for the change of transition states with diffusion length (L_d) and well thickness. Different well widths (3, 4, 5, and 8 nm) with varied L_d are used in the calculation model and the results are shown in the inset of Fig. 2. As L_d increases, the wavelength shifts to shorter wavelength due to group-III interdiffusion. The blueshift rate is faster at same L_d for the thin nanostructure than that for the thick nanostructure. At intermediate stage of intermixing, the disparity in wavelength blueshift is notable. As intermixing proceeds further, the variation rate in wavelength blueshift decreases until the nanostructure is fully intermixed. As a result, with variation in Qdash size, in particular, dash heights as noted in atomic force microscopy data earlier,[2] the broadened linewidth is attributed to the different intermixing results at a medium level of intermixing degree. Furthermore, variation in transition state is more sensitive to the L_d than well width.

Broad area laser characterization further provides evidence of a multistate emission as shown in Fig. 2. A spectral widening is apparent as the bias increases.[11] The emission spectra showing simultaneous two-state lasing emission as injection increases to $1.5J_{th}$ imply the preservation of three-

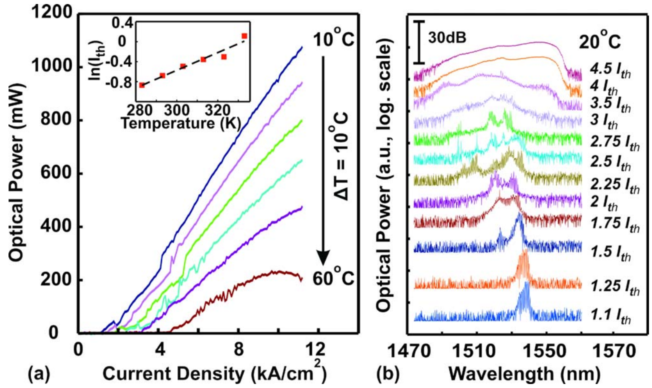

FIG. 3. (Color online) (a) *L-I* characteristics of the 50×500 μm^2 broad area Qdash laser at different temperatures. (b) The lasing spectra are acquired by an optical spectrum analyzer with resolution of 0.05 nm.

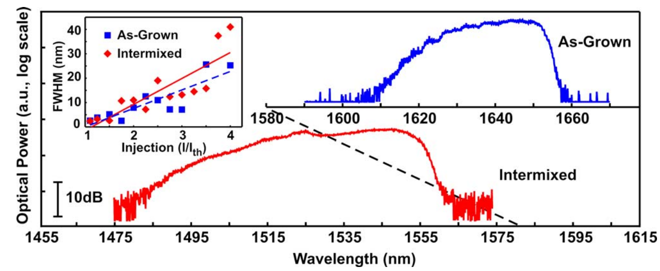

FIG. 4. (Color online) The wavelength tuned broadband Qdash laser from 1.64 to 1.54 μm center wavelength. The lasing coverage increases from 76 to 85 nm after the intermixing process. The inset shows the FWHM of the broadband laser in accordance to injection.

dimensional energy confinement of the Qdash after intermixing. The light-current (*L-I*) curve of the Qdash laser (cavity length $L=500$ μm) yields an improved current density (J_{th}) and slope efficiency of 2.1 kA/cm^2 and 0.423 W/A [Fig. 3(a)] as compared to those of AG laser, which are 2.6 kA/cm^2 and 0.165 W/A, respectively. However, the *L-I* curve of the intermixed laser showing kinks below $\sim$6 kA/cm^2, as compared to the AG laser,[5] implies that the lasing actions from different longitudinal modes and confined energy levels are unstable due to the occurrence of energy exchange between short and long wavelength lasing modes,[11] as can be seen in the lasing spectra of Fig. 3(b). The energy-state hopping instead of mode hopping occurs due to the wide distribution of the energy levels across the highly inhomogeneous Qdash medium, as derived from the PL results. In spite of that, a smooth *L-I* curve above 6 kA/cm^2 yields a total high power of $\sim$1 W per device before thermal rollover. This shows that injection above 6 kA/cm^2 provides enough carriers for population inversion in all the available radiative recombination states, and thus energy-state hopping is absent. Nevertheless, a study on the energy exchange by time resolved spectral measurement[13] instead of average spectra will give a better insight of the Qdash properties, which will be examined and discussed elsewhere.

Measuring the temperature dependence over 10–60 °C reveals the improved temperature characteristic T_o of 56.5 K as compared to the AG laser of 43.6 K.[5] In Fig. 3(b), only a distinctive GS lasing with the wavelength coverage of $\sim$15 nm is observed below injection of $1.5J_{th}$. This broad lasing linewidth suggests collective lasing actions from Qdashes with different geometries. In addition, the supercontinuum lasing spectrum at high current injection ($4J_{th}$) without distinctive gain modulation[9] further validates the postulation of uniform distribution of dash electronic states in a highly inhomogeneous active medium. At $J>1.5J_{th}$, the bistate lasing is evident, which is attributed to the relatively slow carrier relaxation rate and population saturation in the GS. The bistate lasing spectrum is progressively broadened with increasing carrier injection up to a wavelength coverage of 85 nm at $J=4J_{th}$, which is larger than that of AG laser[5] ($\sim$76 nm) (Fig. 4). A center wavelength shift of 100 nm and an enhancement of the broadband linewidth are achieved after the intermediate intermixing. The inset of Fig. 4, showing the changes of FWHM of the broadband laser with injection, depicts that energy-state hopping and multistate lasing emission from Qdashes with different geometries occur.

In conclusion, wavelength tuned broad interband lasers have been fabricated via IFVD to promote group-III intermixing in InAs/InAlGaAs Qdash structure during intermediate stage of intermixing. The intermixed lasers exhibit higher internal quantum efficiency, lower threshold current densities, and larger broad lasing spectra. Bandgap shift of 100 nm has been measured from the intermixed lasers. Our results show that monolithic integration of different gain sections with different bandgaps for ultrabroadband laser is feasible via the intermixing technique. Our results also indicate a highly attractive wavelength trimming method, well suited for improved performance, and planar, monolithic Qdash integration of optoelectronic components.

This work was supported by National Science Foundation (Grant No. 0725647), U.S. Army Research Laboratory, Commonwealth of Pennsylvania, Department of Community and Economic Development. The authors also acknowledge IQE Inc. for the growth of Qdash material.

[1] F. Lelarge, B. Dagens, J. Renaudier, R. Brenot, A. Accard, F. V. Dijk, D. Make, O. L. Gouezigou, J. G. Provost, F. Poingt, J. Landreau, O. Drisse, E. Derouin, B. Rousseau, F. Pommereau, and G. H. Duan, IEEE J. Sel. Top. Quantum Electron. **13**, 111 (2007).
[2] R. H. Wang, A. Stintz, P. M. Varangis, T. C. Newell, H. Li, K. J. Malloy, and L. F. Lester, IEEE Photonics Technol. Lett. **13**, 767 (2001).
[3] H. Dery, E. Benisty, A. Epstein, R. Alizon, V. Mikhelashvii, G. Eisenstein, R. Schwertberger, D. Gold, J. P. Reithmaier, and A. Forchel, J. Appl. Phys. **95**, 6103 (2004).
[4] G. Sek, P. Poloczek, P. Podemski, R. Kudrawiec, J. Misiewicz, A. Somers, S. Hein, S. Hofling, and A. Forchel, Appl. Phys. Lett. **90**, 081915 (2007).
[5] H. S. Djie, C. L. Tan, B. S. Ooi, J. C. M. Hwang, X.-M. Fang, Y. Wu, J. M. Fastenau, W. K. Liu, G. T. Dang, and W. H. Chang, Appl. Phys. Lett. **91**, 111116 (2007).
[6] M. van der Poel, J. Mork, A. Somers, A. Forchel, J. P. Reithmaier, and G. Eisenstein, Appl. Phys. Lett. **89**, 081102 (2006).
[7] C. L. Tan, Y. Wang, H. S. Djie, and B. S. Ooi, Appl. Phys. Lett. **91**, 061117 (2007).
[8] Y. Wang, H. S. Djie, and B. S. Ooi, Appl. Phys. Lett. **88**, 111110 (2006).
[9] L. Harris, D. J. Mowbray, M. S. Skolnick, M. Hopkinson, and G. Hill, Appl. Phys. Lett. **73**, 969 (1998).
[10] H. S. Djie, Y. Wang, Y.-H. Ding, D.-N. Wang, J. C. M. Hwang, X.-M. Fang, Y. Wu, J. Fastenau, A. W. K. Liu, G. T. Dang, W. H. Chang, and B. S. Ooi, IEEE J. Sel. Top. Quantum Electron. **14**, 1239 (2008).
[11] D. Hadass, R. Alizon, H. Dery, V. Mikhelashvili, G. Eisenstein, R. Schwertberger, A. Somers, J. P. Reithmaier, A. Forchel, M. Calligaro, S. Bansropun, and M. Krakowski, Appl. Phys. Lett. **85**, 5505 (2004).
[12] J. H. Wei and K. S. Chan, J. Appl. Phys. **97**, 123524 (2005).
[13] H. Dery and G. Eisenstein, IEEE J. Quantum Electron. **40**, 1398 (2004).